

Clustering features of ${}^9\text{Be}$, ${}^{14}\text{N}$, ${}^7\text{Be}$, and ${}^8\text{B}$ nuclei in relativistic fragmentation

D. A. Artemenkov,* T. V. Shchedrina, R. Stanoeva, and P. I. Zarubin†

Joint Insitute for Nuclear Research, Dubna, Russia

(Dated: November 10, 2021)

Abstract

Recent studies of clustering in light nuclei with an initial energy above 1 A GeV in nuclear track emulsion are overviewed. The results of investigations of the relativistic ${}^9\text{Be}$ nuclei fragmentation in emulsion, which entails the production of He fragments, are presented. It is shown that most precise angular measurements provided by this technique play a crucial role in the restoration of the excitation spectrum of the α particle ssystem. In peripheral interactions ${}^9\text{Be}$ nuclei are dissociated practically totally through the 0^+ and 2^+ states of the ${}^8\text{Be}$ nucleus.

The results of investigations of the dissociation of a ${}^{14}\text{N}$ nucleus of momentum 2.86 A GeV/c in emulsion are presented as example of more complicated system. The momentum and correlation characteristics of α particles for the ${}^{14}\text{N}\rightarrow 3\alpha + X$ channel in the laboratory system and the rest systems of 3α particles were considered in detail.

Topology of charged fragments produced in peripheral relativistic dissociation of radioactive ${}^8\text{B}$, ${}^7\text{Be}$ nuclei in emulsion is studied.

PACS numbers: 21.45.+v, 23.60.+e, 25.10.+s

*Electronic address: artemenkov@lhe.jinr.ru

†Electronic address: zarubin@lhe.jinr.ru; URL: <http://becquerel.lhe.jinr.ru>

I. INTRODUCTION

The peripheral fragmentation of light relativistic nuclei can serve as a source of information about their excitations above particle decay thresholds including many-body final states. The interactions of this type are provoked either in electromagnetic and diffraction processes, or in nucleon collisions at small overlapping of the colliding nucleus densities. A fragmenting nucleus gains an excitation spectrum near the cluster dissociation thresholds. In the kinetic region of fragmentation of a relativistic nucleus there are produced nuclear fragment systems the total charge of it is close to the parent-nucleus charge. A relative intensity of formation of fragments of various configurations makes it possible to estimate the importance of different cluster modes.

The opening angle of the relativistic fragmentation cone is determined by the Fermi-momenta of the nucleon clusters in a nucleus. Being normalized to the mass numbers they are concentrated with a few percent dispersion near the normalized momentum of the primary nucleus. When selecting events with dissociation of a projectile into a narrow fragmentation cone we see that target-nucleus non-relativistic fragments either are absent (“white” stars in Ref.[1]), or their number is insignificant. The target fragments are easily separated from the fragments of a relativistic projectile since their fraction in the angular relativistic fragmentation cone is small and they possess non-relativistic momentum values.

In the peripheral fragmentation of a relativistic nucleus with charge Z the ionization induced by the fragments can decrease down to a factor Z , while the ionization per one track – down to Z^2 . Therefore experiment should provide an adequate detection range. In order to reconstruct an event, a complete kinematic information about the particles in the relativistic fragmentation cone is needed which, e.g., allows one to calculate the invariant mass of the system. The accuracy of its estimation decisively depends on the exactness of the track angular resolution. To ensure the best angular resolution, it is necessary that the detection of relativistic fragments should be performed with the best spacial resolution.

The nuclear emulsion technique, which underlies the BECQUEREL project at the JINR Nuclotron [2], well satisfies the above-mentioned requirements. It is aimed at a systematic search for peripheral fragmentation modes with statistical provision at a level of dozens events, their classification and angular metrology. Emulsions provide the best spacial resolution (about $0.5 \mu\text{m}$) which allows one to separate the charged particle tracks in the

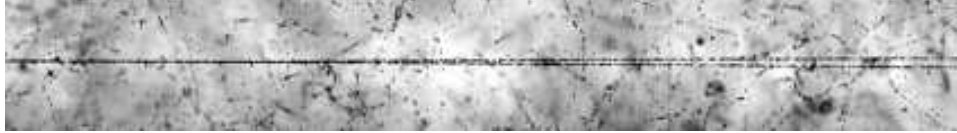


FIG. 1: An event of the type of “white” star from the fragmentation of a relativistic ${}^9\text{Be}$ nucleus into two He fragments in emulsion. The photograph was obtained on the PAVIKOM(FIAN) complex.

three-dimensional image of an event within one-layer thickness ($600\ \mu\text{m}$) and ensure a high accuracy of angle measurements. The tracks of relativistic H and He nuclei are separated by sight. As a rule, in the peripheral fragmentation of a light nucleus its charge can be determined by the sum of the charges of relativistic fragments. Multiple-particle scattering measurements on the light fragment tracks enable one to separate the H and He isotopes. The analysis of the products of the relativistic fragmentation of neutron-deficient isotopes has some additional advantages owing to a larger fraction of observable nucleons and minimal Coulomb distortions. Irradiation details and a special analysis of interactions in the BR-2 emulsion are presented in Ref. [3, 4]. In what follows, we give the first results of the study of the ${}^9\text{Be}$, ${}^8\text{B}$, ${}^7\text{Be}$ ${}^{14}\text{N}$ nuclei fragmentation with a few A GeV energy which are obtained with the use of a part of the material analyzed.

II. FRAGMENTATION OF ${}^9\text{Be}$ NUCLEI

The ${}^9\text{Be}$ nucleus is a loosely bound $n+\alpha+\alpha$ system. The energy threshold of the ${}^9\text{Be}\rightarrow n+\alpha+\alpha$ dissociation channel is 1.57 MeV. The study of the ${}^9\text{Be}$ fragmentation at relativistic energies gives the possibility of observing the reaction fragments, which are the decay products of unbound ${}^8\text{Be}$ and ${}^5\text{He}$ nuclei.

The method of nuclear emulsions used in the present paper allows one to observe the charged component of the relativistic ${}^9\text{Be}\rightarrow 2\text{He}+n$ fragmentation channel. Owing to a good angular resolution of this method it is possible to separate the ${}^9\text{Be}$ fragmentation events, which accompanied by the production of an unstable ${}^8\text{Be}$ nucleus with its subsequent breakup to two α particles. In this case, the absence of a combinatorial background (of three and more α particles) for ${}^9\text{Be}$, which is typical for heavier $N\alpha$ nuclei ${}^{12}\text{C}$ and ${}^{16}\text{O}$ makes it possible to observe distinctly this picture.

Nuclear emulsions were exposed to relativistic ${}^9\text{Be}$ nuclei at the JINR Nuclotron. A

beam of relativistic ${}^9\text{Be}$ nuclei was obtained in the ${}^{10}\text{B}\rightarrow{}^9\text{Be}$ fragmentation reaction using a polyethylene target. The ${}^9\text{Be}$ nuclei constituted about 80% of the beam, the remaining 20% fell on Li and He nuclei.[5]

Events were sought by microscope scanning over the emulsion plates. In total 362 events of the ${}^9\text{Be}$ fragmentation involving the two He fragment production in the forward fragmentation cone within a polar angle of 6° (0.1 rad) were found. The requirement of conservation of the fragment charge in the fragmentation cone was fulfilled for the detected events. In event selection 5 - 7 tracks of various types were allowed in a wide (larger than 6°) cone to increase statistics. An example of the ${}^9\text{Be}\rightarrow 2\text{He}$ fragmentation event in emulsion is given in Fig. 1 [2]. This event belongs to the class of “white” stars as far as it contains neither target nucleus fragments, nor produced mesons. This event sample includes 144 “white” stars. The angles of the tracks in emulsion for the detected events were obtained using a fine measuring microscope. Angular measurements for the 362 events were carried out with an accuracy not worse than 4.5×10^{-3} rad.

In analyzing the data both He fragments observed in the ${}^9\text{Be}\rightarrow 2\text{He}+n$ channel were supposed to be α particles. This assumption is motivated by the fact that at small angles the ${}^9\text{Be}\rightarrow 2{}^4\text{He}+n$ fragmentation channel with an energy threshold of 1.57 MeV must dominate the ${}^9\text{Be}\rightarrow {}^3\text{He}+{}^4\text{He}+n$ channel whose energy threshold is 22.15 MeV. The ${}^3\text{He}$ fraction will not exceed a few percent in this energy range [6] and all the He fragments in the detected events may be thought of as α particles.

In Fig. 2a the P_T transverse momentum distribution of α particles in the laboratory frame of reference is calculated without the account of particle energy losses in emulsion by the equation

$$P_T = p_0 \cdot A \cdot \sin\theta \quad (1)$$

where p_0 , A and θ are the momentum per nucleon, the fragment mass and the polar emission angle, respectively. The outer contour corresponds to all events. The inner histogram is obtained for events accompanied by protons recoil of emulsion target (dashed area). The mean value of the transverse momentum for the total event sample in the laboratory system is equal to $\langle P_T \rangle \approx 103$ MeV/c with FWHM $\sigma \approx 72$ MeV/c. This may be an indication of the fact that the experimental data are not of the same kind which can be pronounced when going over to the c.m.s. of two α particles.

The P_T^* transverse momentum distribution of α particles in the c.m.s. of two α particles

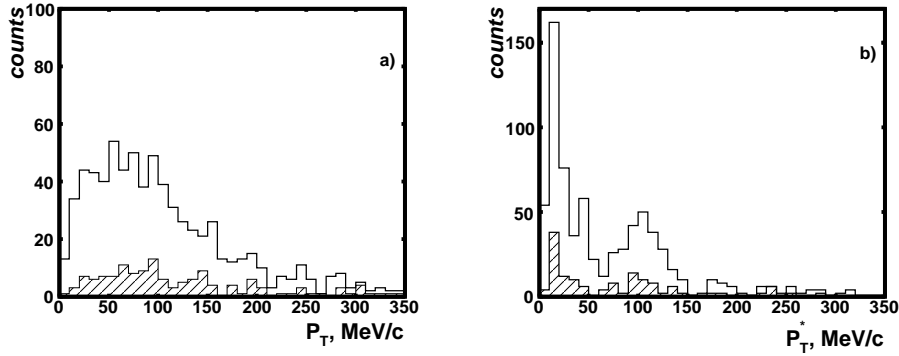


FIG. 2: The P_T transverse momentum distribution of α particles in the laboratory system (a), and the P_T^* momentum distribution in the c.m.s. of an α particle pair (b). The outer contour corresponds to all events. The inner histogram is obtained for events, which accompanied by protons recoil of emulsion target (dashed area).

described by the equation

$$\mathbf{P}_{T_i}^* \cong \mathbf{P}_{T_i} - \frac{\sum_{i=1}^n \mathbf{P}_{T_i}}{n_\alpha} \quad (2)$$

where P_{T_i} is the transverse momentum of an i -th α particle in the laboratory system $n_\alpha=2$ is given in Fig. 2b. There is observed a grouping of events around two peaks with the values $\langle P_{T_i}^* \rangle \approx 24$ MeV/c and $\langle P_{T_i}^* \rangle \approx 101$ MeV/c. In Ref [7] the appropriate mean values of the α fragment transverse momenta are $\langle P_{T_i}^* \rangle \approx 121$ MeV/c for $^{16}\text{O} \rightarrow 4\alpha$, $\langle P_{T_i}^* \rangle \approx 141$ MeV/c [8] for $^{12}\text{C} \rightarrow 3\alpha$ and $\langle P_{T_i}^* \rangle \approx 200$ MeV/ for $^{22}\text{Ne} \rightarrow 5\alpha$ (processing of the available data). There by we clearly see a tendency toward an increase of the mean α particle momentum with increasing their multiplicity. This implies a growth of the total Coulomb interaction of alpha clusters arising in nuclei.

In the opening angle Θ distribution (Fig. 3) one can also see two peaks with mean values 4.6×10^{-3} rad. and 26.8×10^{-3} rad. The ratio of the numbers of the events in the peaks is close to unity.

The Θ distribution entails the invariant energy $Q_{2\alpha}$ distribution, which is calculated as a difference between the effective invariant mass $M_{2\alpha}$ of an α fragment pair and the doubled α particle mass by the equations

$$M_{2\alpha}^2 = -\left(\sum_{j=1}^2 P_j\right)^2$$

$$Q_{2\alpha} = M_{2\alpha} - 2 \cdot m_\alpha \quad (3)$$

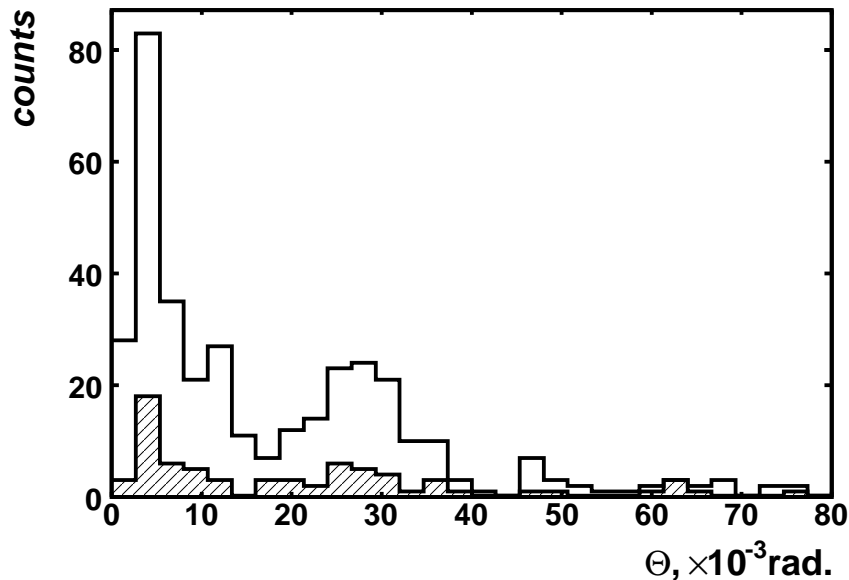


FIG. 3: The opening Θ angle distribution of α particles in the ${}^9\text{Be} \rightarrow 2\alpha$ fragmentation reaction at 1.2 A GeV energy. The outer contour corresponds to all events. The inner histogram is obtained for events, which accompanied by protons recoil of emulsion target (dashed area).

where P_j is the α particle 4-momentum.

In the invariant energy $Q_{2\alpha}$ distribution (Fig. 4) there are two peaks in the ranges 0 to 1 MeV and 2 to 4 MeV. The shape of the distribution does not contradict the suggestion about the ${}^9\text{Be}$ fragmentation involving the production of an unstable ${}^8\text{Be}$ nucleus which decays in the 0^+ and 2^+ states. The values of the peaks of the invariant energy $Q_{2\alpha}$ and the transverse momenta P_T^* in the c.m.s. relate to each other. To the $Q_{2\alpha}$ range from 0 to 1 MeV with a peak at 100 keV there corresponds a peak P_T^* with $\langle P_{T_i}^* \rangle \approx 24$ MeV/c, and to the $Q_{2\alpha}$ range from 2 to 4 MeV there corresponds a peak with $\langle P_{T_i}^* \rangle \approx 101$ MeV/c.

III. FRAGMENTATION OF ${}^{14}\text{N}$ NUCLEI

A stack of layers of BR-2 emulsion was exposed to a beam of ${}^{14}\text{N}$ nuclei accelerated [9] to a momentum of 2.86 A GeV/c at the Nuclotron of the Laboratory of High Energy Physics (JINR). Already been found among 950 inelastic events in which the total fragment charge was equal to the $Z_0=7$ fragment charge and there were no produced particles. Events were sought by viewing over the track length which provided the accumulation of statistics

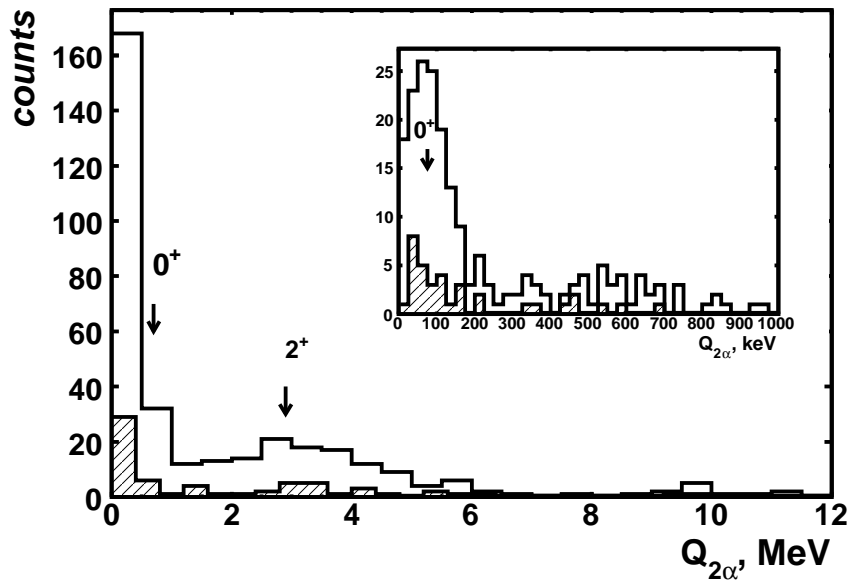


FIG. 4: The invariant energy $Q_{2\alpha}$ distribution of α particle pairs in the ${}^9\text{Be} \rightarrow 2\alpha$ fragmentation reaction at 1.2 A GeV energy. On the intersection: the $Q_{2\alpha}$ range from 0 to 1 MeV. Arrows mark the ${}^8\text{Be}$ nucleus levels (0^+ and 2^+). The outer contour corresponds to all events. The inner histogram is obtained for events, which accompanied by protons recoil of emulsion target (dashed area).

without selection. The selected events are divided in two classes. The events of the type of “white”star and the interactions involving the production of one or a few target-nucleus fragments belong to the first class.

Table I shows the charge multi-fragmentation topology which was studied for the events satisfying the above-mentioned conditions. The upper line is the $Z > 2$ fragment charge, the second line is the number of single-charged fragments, the third one the number of two-charged fragments, and the fourth and fifth lines are the number of the detected events with a given topology for “white”stars and events with target-nucleus excitation for each channel, respectively. The two last lines present the total number of interactions calculated in absolute values and in percent.

The analysis of the data of Table I shows that the number of channels involving $Z > 3$ fragments for the “white”stars is larger by about a factor of 1.5 than that for the events accompanied by a target breakup. On the contrary, for the 2+2+2+1 charge configuration

TABLE I: The charge topology distribution of the “white” stars and the interactions involving the target-nucleus fragment production in the ^{14}N dissociation at 2.86 A GeV/c momentum.

Z_{fr}	6	5	5	4	3	3	–	–
$N_{Z=1}$	1	–	2	1	4	2	3	1
$N_{Z=2}$	–	1	–	1	–	1	2	3
$N_{W.S.}$	13	4	3	1	1	1	6	17
$N_{t.f.}$	15	1	3	3	–	2	5	32
N_{Σ}	28	5	6	4	1	3	11	49
$N_{\Sigma,\%}$	26	5	5	4	1	3	10	46

channel this number is smaller by about a factor of 1.5. Thus, in the events with target breakup, the projectile fragments more strongly than in the “white” stars. The data of Table I points to the predominance of the channel with the 2+2+2+1 charge configuration (49 events) which has been studied in more detail. The obtained results show that the ^{14}N nucleus constitutes a very effective source for the production of 3α system.

In order to estimate the energy scale of production of 3α particle systems in the $^{14}\text{N}\rightarrow 3\alpha + X$ channel, we present the invariant excitation energy $Q_{3\alpha}$ distribution with respect to the ^{12}C ground state:

$$M_{3\alpha}^2 = -\left(\sum_{j=1}^3 P_j\right)^2$$

$$Q_{3\alpha} = M_{3\alpha}^* - M(^{12}\text{C}) \quad (4)$$

where $M(^{12}\text{C})$ is the mass of the ground state corresponding to the charge and the weight of the system being analyzed, $M_{3\alpha}^*$ the invariant mass of the system of fragments. Statistics was increased to 132 events $^{14}\text{N}\rightarrow 3\alpha + X$ including 50 “white” stars by scanning over the emulsion plates.

The main part of the events is concentrated in the $Q_{3\alpha}$ area from 10 to 14 MeV, covering the known ^{12}C levels (Fig. 5). Softening of the conditions of the $3\text{He} + \text{H}$ selection, for which the target fragment production is allowed, does not result in a shift of the 3α excitation peak. This fact suggests the universality of the 3α state population mechanism.

To estimate the fraction of the events involving the production of an intermediate ^8Be nucleus in the reactions $^{14}\text{N}\rightarrow ^8\text{Be} + X \rightarrow 3\alpha + X$ we present the invariant excitation energy

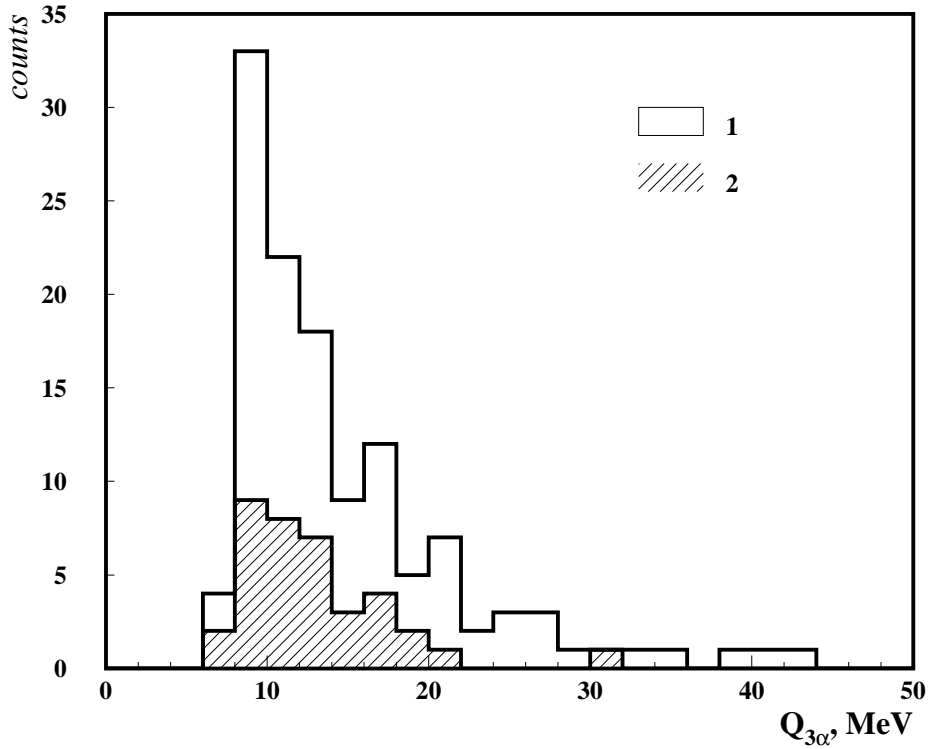


FIG. 5: The invariant excitation energy $Q_{3\alpha}$ distribution of three α particles with respect to the ^{12}C ground state for the process $^{14}\text{N} \rightarrow 3\alpha + X$. The following notation is used: 1) all the events of the given dissociation, 2) “white” stars.

distribution for an α particle pair with respect to the ^8Be ground state (Fig. 6). The first distribution peak relates to the value to be expected for the decay products of an unstable ^8Be nucleus in the ground state 0^+ . The distribution centre is seen to coincide well with the decay energy of the ^8Be ground state. The fraction of the α particles originating from the ^8Be decay is 25-30%.

IV. FRAGMENTATION OF ^7Be , AND ^8B NUCLEI

The results of investigations dealing with the charge topology of the fragments produced in peripheral dissociation of relativistic ^8B , ^7Be nuclei in emulsion are presented in Ref [2, 10, 11, 12].

Table II presents the numbers of the events detected in various channels of the ^7Be

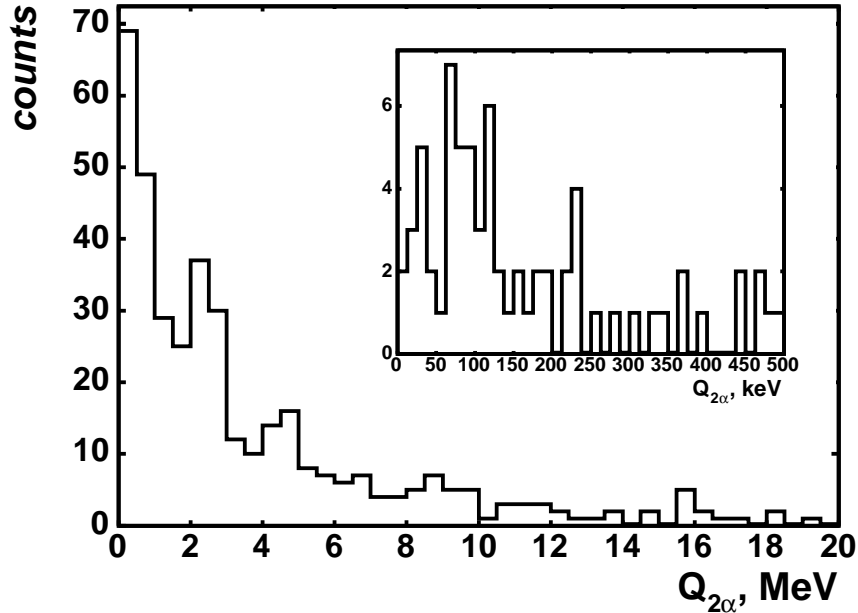


FIG. 6: The invariant excitation energy $Q_{2\alpha}$ distribution of α particle pairs for the process $^{14}\text{N} \rightarrow 3\alpha + X$. In the inset: a fraction of the distribution at 0-500 keV.

fragmentation. Of them, the $^3\text{He} + ^4\text{He}$ channel noticeably dominates, the channels $^4\text{He} + d + p$ and $^6\text{Li} + p$ constitute 10% each. Two events involving no emission of neutrons in the three-body channels $^3\text{He} + t + p$ and $^3\text{He} + d + d$ were registered. The reaction of charge-exchange of ^7Be nuclei to ^7Li nuclei was not detected among the events not accompanied by other secondary charged particles. The events involving no target fragments ($n_b = 0$) are separated from the events involving one or a few fragments ($n_b > 0$).

For the first time, nuclear emulsions were exposed to a beam of relativistic ^8B nuclei. We have obtained data on the probabilities of the ^8B fragmentation channels in peripheral interactions. 55 events of the peripheral ^8B dissociation which do not involve the production of the target-nucleus fragments and mesons (“white” stars) were selected. A leading contribution of the $^8\text{B} \rightarrow ^7\text{Be} + p$ mode having the lowest energy threshold was revealed on the basis of these events. Information about a relative probability of dissociation modes with larger multiplicity have been obtained. Among the found events there are 320 stars in which the total charge of the relativistic fragments in a 8° fragmentation cone $\sum Z_{fr}$ satisfies the condition $\sum Z_{fr} > 3$. These stars were attributed to the number of peripheral dissociation events N_{pf} . The N_{pf} relativistic fragment distribution of over charges N_Z is given in

TABLE II: ${}^7\text{Be}$ fragmentation channel (number of events)

Channel	2He		He+2H		4H		Li+H		Sum
	$n_b = 0$	$n_b > 0$	$n_b = 0$	$n_b > 0$	$n_b = 0$	$n_b > 0$	$n_b = 0$	$n_b > 0$	
${}^3\text{He}+{}^4\text{He}$	30	11							41
${}^3\text{He}+{}^3\text{He}$	11	7							18
${}^4\text{He}+2\text{p}$			13	9					22
${}^4\text{He}+\text{d}+\text{p}$			10	5					15
${}^3\text{He}+2\text{p}$			9	9					18
${}^3\text{He}+\text{d}+\text{p}$			8	10					18
${}^3\text{He}+2\text{d}$			1						1
${}^3\text{He}+\text{t}+\text{p}$			1						1
$3\text{p}+\text{d}$					2				2
$2\text{p}+2\text{d}$					1				1
${}^6\text{Li}+\text{p}$							9	3	12
Sum	41	18	42	33	2	1	9	3	149

Table III. There are given the data for 256 events containing the target-nucleus fragments - N_{tf} , as well as for 64 events which contain no target-nucleus fragments (“white” stars) - N_{pf} . The role of the channels with multiple relativistic fragments $N_Z > 2$ is revealed to be dominant for the N “white” stars. Of peripheral events, the “white” stars N_{ws} (Table III) are of very particular interest. They are not accompanied by the target-nucleus fragment tracks and makes it possible to clarify the role of different cluster degrees of freedom at a minimal excitation of the nuclear structure.

Table IV gives the relativistic fragment charge distribution in the “white” stars for ${}^7\text{Be}$ and ${}^8\text{B}$ nuclei. The ${}^8\text{B}$ events are presented without one single-charged relativistic fragment, that is a supposed proton halo. The identical fraction of the two main 2He and He+2H dissociation channels is observed for ${}^7\text{Be}$ and ${}^8\text{B}$ nuclei which points out that the ${}^8\text{Be}$ core excitation is independent of the presence of an additional loosely bound proton in the ${}^8\text{B}$ nucleus.

TABLE III: The charge topology distribution of the number of interactions of the peripheral N_{pf} type ($N_{pf}=N_{tf}+N_{ws}$), which were detected in an emulsion exposed to a second ^8B nucleus beam. Here Z_{fr} is the total charge of relativistic fragments in a 8° angular cone in an event, N_Z the number of fragments with charge Z in an event, N_{ws} the number of “white” stars, N_{tf} the number of events involving the target fragments, N_{ws} the number of “white” stars.

Z_{fr}	N_5	N_4	N_3	N_2	N_1	N_{tf}	N_{ws}
7	-	-	-	1	5	1	-
6	-	-	-	2	2	8	2
6	-	-	-	1	4	6	4
6	-	-	-	-	6	1	-
5	-	-	-	1	3	61	14
5	-	-	-	2	1	44	12
5	-	-	1	-	2	8	-
5	-	-	1	1	-	1	-
5	-	1	-	-	1	17	24
5	1	-	-	-	-	17	1
5	-	-	-	-	5	21	4
4	-	-	-	-	4	5	1
4	-	-	-	2	-	24	1
4	-	-	-	1	2	42	-

TABLE IV: The charged dissociation mode distribution of the “white” stars produced by the ^7Be and ^8B nuclei. To make the comparison more convenient, for the ^8B nucleus one H nucleus is eliminated from the charged mode and the channel fractions are indicated.

$\Sigma Z_{fr}=4$	^7Be	%	^8B (+H)	%
2He	41	43	12	40
He+2H	42	45	14	47
4H	2	2	4	13

V. CONCLUSIONS

The degree of the dissociation of the relativistic nuclei in peripheral interactions can reach a total destruction into nucleons and singly and doubly charged fragments. The emulsion technique allows one to observe these systems to the smallest details and gives the possibility of studying them experimentally.

New experimental observations are reported from the emulsion exposures to ^{14}N , ^9Be , ^8B , ^7Be nuclei with energy above 1 A GeV. The main features of $^9\text{Be}\rightarrow 2\text{He}$ relativistic fragmentation are presented. For the particular case of the relativistic ^9Be nucleus dissociation it is shown that precise angular measurements play a crucial role in the restoration of the excitation spectrum of the alpha particle fragments. This nucleus is dissociated practically totally through the 0^+ and 2^+ states of the ^8Be nucleus. The data obtained from ^9Be angular measurements can be employed for the estimation of the role of ^8Be in more complicated $\text{N}\alpha$ systems.

The results of the study of the dissociation of ^{14}N nuclei of a primary momentum of 2.86 A GeV/c in their interactions with the emulsion nuclei are also presented. The present investigation indicates the leading role of the $2+2+2+1$ charge configuration channel. The energy scale of the 3α system production has been estimated. According to the available statistics 80% of interactions are concentrated at 10-14 MeV. The fraction of the $^{14}\text{N}\rightarrow ^8\text{Be}+\text{X}\rightarrow 3\alpha+\text{X}$ channel involving the production of an intermediate ^8Be nucleus is about 25%.

Advantages of emulsion technique are exploited most completely in the study of peripheral fragmentation of light stable and neutron deficient nuclei. The results of investigations dealing with the charge topology of the fragments produced in peripheral dissociation of relativistic ^7Be , ^8B nuclei in emulsion are presented. Information on the relative probability of dissociation modes with a larger multiplicity was obtained. The dissociation of a ^7Be core in ^8B indicates an analogy with that of the free ^7Be nucleus.

-
- [1] N. P. Andreeva, et al., *Phys. At. Nucl.* **68**, 455–465 (2005).
- [2] Web site of the BECQUEREL Project: <http://becquerel.jinr.ru> (2006).
- [3] M. I. Adamovich, et al., *Phys. At. Nucl.* **62**, 1378–1387 (1999).
- [4] M. I. Adamovich, et al., *Phys. At. Nucl.* **62**, 514–517” (2004).
- [5] D. A. Artemenkov, arXiv:nucl-ex/0605018 (2006).
- [6] V. V. Belaga, et al., *Phys. At. Nucl.* **59**, 869–877 (1996).
- [7] F. A. Avetyan, et al., *Phys. At. Nucl.* **59**, 110–116 (1996).
- [8] V. V. Belaga, et al., *Phys. At. Nucl.* **58**, 2014–2020 (1995).
- [9] T. V. Shchedrina, et al., arXiv:nucl-ex/0605022 (2006).
- [10] R. Stanoeva, et al., arXiv:nucl-ex/0605013 (2006).
- [11] N. G. Peresadko, et al., arXiv:nucl-ex/0605014 (2006).
- [12] N. P. Andreeva, et al., arXiv:nucl-ex/0604003 (2006).